Nov 10th, 12:00 AM - 12:00 AM

Behaviour of Cold-Formed Steel Trusses with Concentric and Eccentric Joint Arrangements using the Howick Rivet Connector

Amin Ahmadi

Colin K. L. Yee

Harry J. S. Shepherd

G. Charles Clifton

Raj Das

See next page for additional authors

Wei-Wen Yu International Specialty Conference on Cold-Formed Steel Structures
Baltimore, Maryland, U.S.A, November 9 & 10, 2016

Behaviour of cold-formed steel trusses with concentric and eccentric joint arrangements using the Howick Rivet Connector

Amin Ahmadi[1], Colin K.L. Yee[2], Harry J. S. Shepherd[2], G. Charles Clifton[3], Raj Das[4] and James B.P. Lim[4]

Abstract

This paper considers the behaviour of a cold-formed steel truss system that uses a novel pinned connector for the joints, to be referred to as the Howick Rivet connector (HRC). Use of the HRC allows a pinned concentric joint arrangement to be formed, as well as the more usual eccentric joint arrangement used in tests described in the literature. However, with the concentric joint arrangement, it is necessary to remove part of the lips of the channel-sections being connected, thus creating a discontinuity in the lips. This paper assesses the effect of this discontinuity. Full-scale truss tests are first described. The trusses have span of 6 m, depth of 1.8 m and length of diagonals of 2.3 m; both pinned concentric and pinned eccentric joint arrangement are tested. It was shown that the mid-span deflection of the concentric joint arrangement in the elastic range is 3 times smaller and 64% stiffer than that of the eccentric joint arrangement; the overall failure loads, due to flexural-torsional buckling of the diagonal members, were found to be similar, and were not influenced by removal of part of the lips of the channel-sections. To investigate the effect of removing the lips for the concentric joint arrangement, a series of truss panel tests were performed for which the length of the diagonals were 0.6 m. Failure was found to be localised buckling at the discontinuity where the lips were removed.

1 Introduction

The authors have recently described a novel pinned connector, to be referred to as Howick Rivet Connector (HRC) [1, 2] (see Fig. 1), that can be used as an alternative to bolts or self-drilling screws. As can be seen in Fig. 1, the HRC

comprises a hollow-tubed rivet with a set of inner and outer swaged collars at each end. The HRC has a diameter of 12.70 mm and thickness of 0.95 mm. Compared with traditional connections, HRC has no initial slip and so a higher proportionality limit; furthermore installation of the HRC requires only a single operation, resulting in cost savings in labour. This paper considers the application of the HRC to cold-formed steel truss systems.

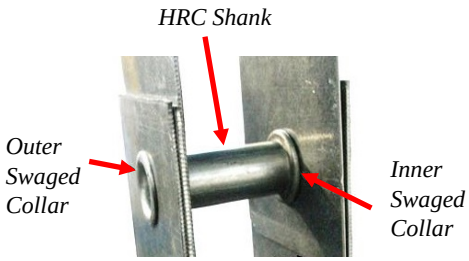

Figure 1: Photograph of Howick Rivet Connector

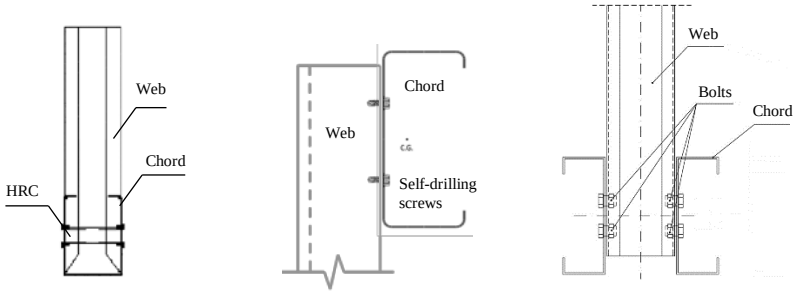

a. HRC joint arrangement of truss

b. Laboube and his co-workers [3, 4, 5]

c. Zaharia and Dubina [6]

Figure 2: Joint arrangement of trusses

Details of the cold-formed steel joint arrangement used by the HRC for trusses are shown in Fig. 2a. As can be seen, the joint arrangement comprises the HRC, web and chord members where the diagonal (web) member nest into the chord

member; the sections are connected through the flanges by the HRC. For comparison, details of the other joint arrangements that have been described in the literature for cold-formed steel trusses are shown in Fig. 2b and c; these pertain to experimental tests by LaBoube and his co-workers [3, 4, 5] and Zaharia and Dubina [6], respectively.

It can be seen from Fig. 2a, that the joint arrangement used by the HRC for trusses differs from the other two joint arrangements. The joint arrangement described by LaBoube (see Fig. 2b) used back-to-back channel-sections connected using self-drilling screws, while that of Zaharia and Dubina [6] (see Fig. 2c) used diagonal members sandwiched between the chord member on both sides and connected using bolts.

Moreover, the HRC permits either a concentric or an eccentric joint arrangement to be formed, unlike that of the joint arrangements of LaBoube and his co-workers and Zaharia and Dubina which only permit eccentric joint arrangements. The concentric joint arrangement, however, requires the lip of a web member to be removed near to the joint at one end of each web member, as can be seen in Fig. 3, which will have an effect on the compression capacity of the web diagonal member. The eccentric joint arrangements does not require the lip to be removed for the web member. The lip of the chord member in both cases is folded inwards (see Fig. 3).

Figure 3: Concentric joint arrangement used by the HRC

This paper describes full scale tests on the HRC truss arrangement for both concentric and eccentric joint arrangements. The truss specimens considered have a span of 6 m and a depth of 1.8 m.

2 Experimental Investigation

2.1 Full-scale truss tests

2.1.1 Details of specimens

For concentrically jointed truss, due to discontinuity in the lip, the truss assembly was designed large enough to ensure that the diagonals would fail through flexural-torsional buckling. Such an approach would be expected to eliminate the effect of localised buckling of the discontinuity. Hence, the effect of eccentricity of the connections on the truss system would be the aim of the study. Details of the concentric and eccentric joint arrangements for the truss specimens are shown in Fig. 4. As can be seen, the length of each truss was 6 m and the depth was 1.8 m; the length of the diagonal (L_d) was 2.343 m and 2.288 m for the concentric and eccentric joint arrangements, respectively.

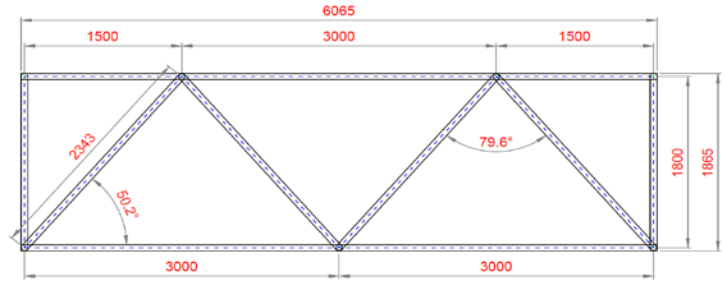

a. Concentric joint arrangement

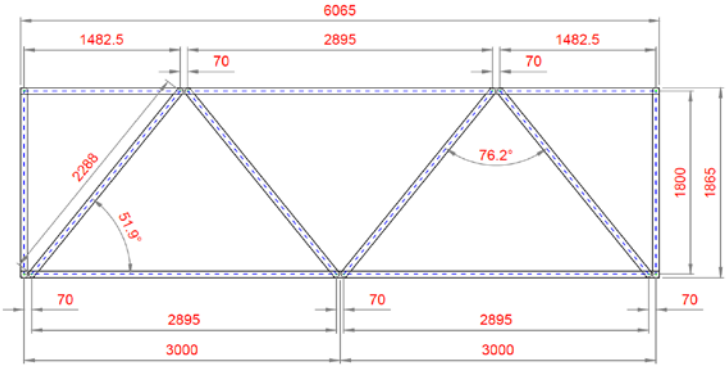

b. Eccentric joint arrangement

Figure 4: Full-scale truss specimen details

Six tests were conducted in total, three for the concentrically jointed truss and three for the eccentrically jointed truss. For the case of the eccentric joint arrangement used for the truss, the distance between the HRCs was 70 mm. All the trusses were fabricated with the centre of the holes located at the centre of the flange of the chord. Fig. 5 shows the specimen labelling convention for the truss specimens.

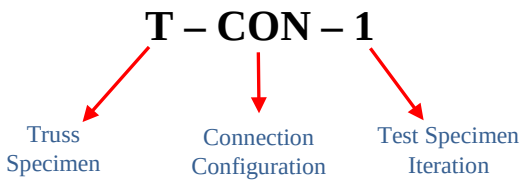

Figure 5: Truss specimen labeling convention

The chord and web members are assembled from a channel section having nominal dimensions of 45 mm x 65 mm x 10 mm x 0.95 mm, referring to the web, flange, lip and thickness, respectively.

2.1.2 Material properties

A set of coupon tests were carried out in order to determine the tensile properties of the materials. All tests were implemented according to ISO 6892-1:2009 [7]. The nominal yield stress of the channel sections was 550 MPa. For the ply material, three coupons were obtained in the longitudinal orientation and tested using Instron Universal Testing Machine. Two portal gauges were placed on the left and the right sides of the specimens to measure the elongation during the test and to ensure no bending moment is generated due to the eccentricity. The material properties and average test results are summarized in Table 1.

Table 1: Material properties of channel-sections (E = 230 GPa)

Nominal Thickness (mm)	Base Metal* Thickness (mm)	Gauge Width (mm)	Gauge Length (MPa)	Yield Stress** (MPa)	Tensile Stress (MPa)	Elongation At Rupture (%)
0.95	0.91	20	140	717	700	1.7

*Base Metal thickness refers to ply thickness without galvanized (zinc) coating.
**This is the upper yield stress.

Three tensile tests were also conducted for the HRC in the longitudinal direction. The HRC hollow tube was plugged at both ends so they could be gripped using conical grips. The relative displacement was measured by two portal gauges; one on each side. The average test result is shown in Table 2. The base metal thickness of ply and HRC was used for calculation of the stresses, which excludes the galvanised coating thickness determined according to AS 1397 [8].

Table 2: Material properties of HRC

HRC Specimen	Base Metal* Thickness (mm)	Outside Diameter (mm)	Gauge Length (mm)	Yield Stress (MPa)	Tensile Stress (MPa)	Elongation At Rupture (%)
12.70x0.95	0.91	12.70	300	480	500	2.8

*Base Metal thickness refers to ply thickness without galvanized (zinc) coating.

2.1.3 Test rig and procedure

Fig. 6 shows the four-point bending test set-up. Two sets of steel dual-columns at ¼ and ¾ truss span provided points of attachment for the hydraulic actuators and top chord lateral supports (see Fig. 6c). Steel platforms at each end of the truss provided a simple support condition, and also laterally supported the truss at those locations (see Fig. 6a). A central platform (see Fig. 6b) was used to provide lateral support for the bottom chord, and a point of attachment for a linear variable differential transformer (LVDT).

For all tests, loading point and mid-span deflection measurements were recorded; the latter with a LVDT at the midpoint of the bottom chord (see Fig. 6b). Static loading was applied using a pair of 30-ton hydraulic actuators. These were suspended vertically from the tops of the dual-columns (see Fig. 6c) and operated manually using hand-jacks. As each jack was loaded manually, care was taken to ensure that the loads were close to equal. The instantaneous load readings from the load cells were used to control the magnitude and rate of loading during testing.

All truss specimens were braced against out-of-plane movement at 3 m by the installation of lateral supports installed at the 5 joint locations, i.e. at the supports, at the mid-span and at the hydraulic actuators. During testing, the actuator load was increased at 0.5 kN intervals, until ultimate failure of the truss specimens occurred. Once the load increment was achieved, it was held constant for a

minimum of 60 seconds, and load and deflection measurements were taken at the end of this period.

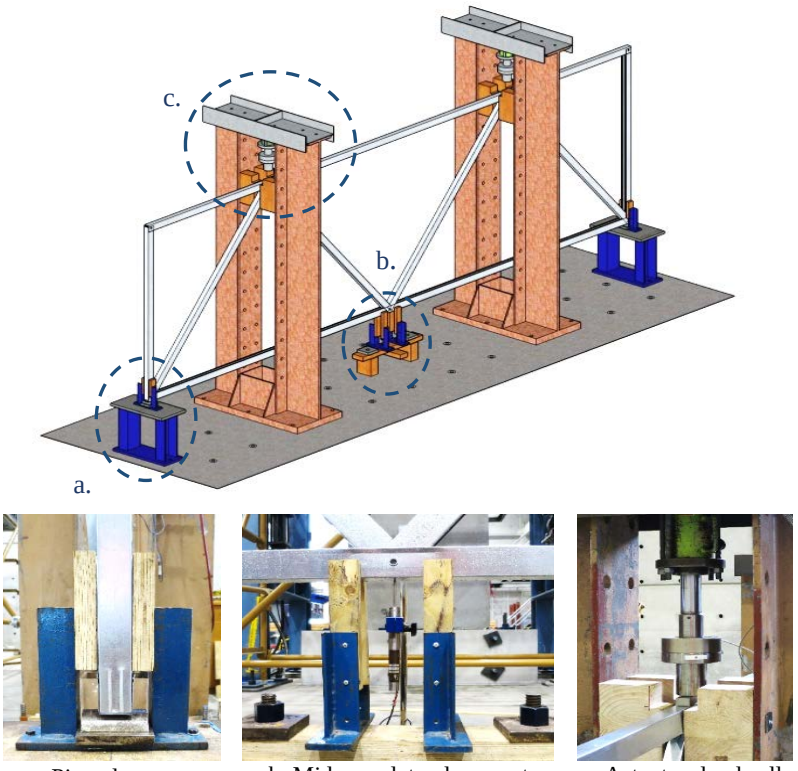

a. Pinned support detail

b. Mid-span lateral support and LVDT

c. Actuator, load cell and top-chord lateral support

Figure 6: Test rig of full-scale truss test

2.1.4 Test results

Fig. 7 shows the variation of total load against mid-span deflection for the trusses. Fig. 8 shows the mode of failure of diagonal members, which is through flexural-torsional buckling. Neither deformation nor failure of the HRC connection was observed in any of the specimens. Table 3 shows the experimental peak loads

(P_{EXP}) for the concentric and eccentric joint arrangements. The peak load refers to the maximum axial compression load in a single diagonal member before failure.

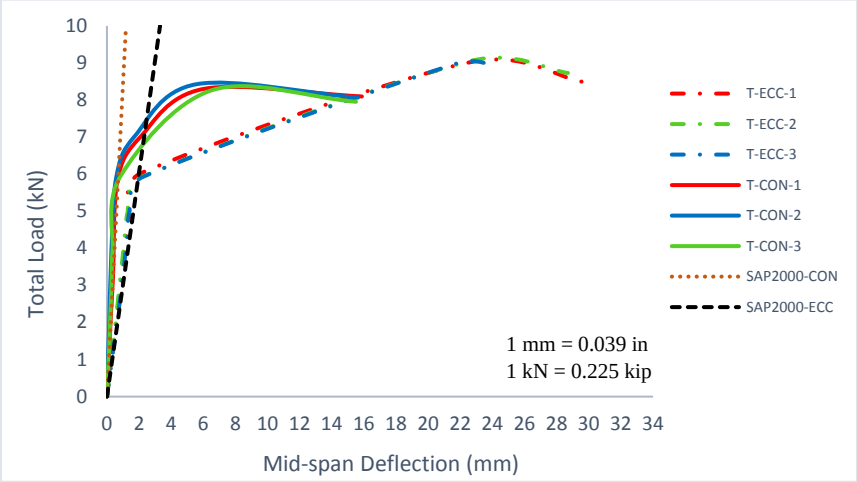

Figure 7: Total load against mid-span deflection for trusses

a. Flexural-torsional buckling

b. Damage to the flange and web

c. Lip and flange after the failure

Figure 8: Critical diagonal member failure modes

As can be seen from Fig. 7, the elastic stiffness of the truss with the concentric joint arrangement was 64% higher than that of the truss with the eccentric joint arrangement. While the truss with the concentric joint arrangement failed at a load of 11% lower than that of the truss with the eccentric joint arrangement, this can be attributed to the different length of diagonal members, with the length of the diagonal members (L_d) being 2343 mm and 2288 mm for the truss with the concentric and the eccentric joint arrangement, respectively. The mid-span deflection of the concentrically jointed arrangement in the elastic range is 3 times smaller than that of the eccentrically jointed truss. All truss specimens failed in flexural-torsional buckling of the outer diagonal members.

Table 3: Experimental results from full-scale truss test

a. Concentric joint arrangement (L_d = 2343 mm)

No	Test Specimen	DSM Result Without Lip P_{DSM-N} kip (kN)	DSM Result With Lip P_{DSM-L} kip (kN)	Total Load P_{TEXP} (kN)	Mid-span Deflec. Δ (mm)	Mean Mid-span Deflec. Δ_{EXP} (mm)	Load in a Single Member P_{EXP} (kN)	Mean Peak Load P_{mEXP} kip (kN)	Variation η (%)	P_{EXP}/P_{DSM-N}	P_{EXP}/P_{DSM-L}	Mode of Failure
1	T-CON-1	3.01	5.49	8.30	6.04	6.07	5.40	5.42	0.38	1.79	0.98	F-T Buckling
2	T-CON-2			8.43	5.59		5.48		1.14	1.82	1.00	F-T Buckling
3	T-CON-3			8.27	6.57		5.38		0.76	1.79	0.98	F-T Buckling
Mean P_m										1.802	0.988	
Mean Standard Deviation										0.018	0.010	
Coefficient of Variation, V_p										0.010	0.010	

b. Eccentric joint arrangement (L_d = 2288 mm)

No	Test Specimen	DSM Result Without Lip P_{DSM-N} (kN)	DSM Result With Lip P_{DSM-L} (kN)	Total Load P_{TEXP} (kN)	Mid-span Deflec. Δ (kN)	Mean Mid-span Deflec. Δ_{EXP} (kN)	Load in a Single Member P_{EXP} (kN)	Mean Peak Load P_{mEXP} (kN)	Variation η (%)	P_{EXP}/P_{DSM-N}	P_{EXP}/P_{DSM-L}	Mode of Failure
1	T-ECC-1	3.19	5.76	9.01	22.56	22.33	6.02	6.02	0.06	1.89	1.05	F-T Buckling
2	T-ECC-2			9.05	22.56		6.03		0.11	1.89	1.05	F-T Buckling
3	T-ECC-3			9.00	21.87		6.02		0.06	1.89	1.05	F-T Buckling
Mean P_m										1.888	1.046	
Mean Standard Deviation										0.002	0.001	
Coefficient of Variation, V_p										0.001	0.001	

2.2 Truss panel test for truss with concentric joint arrangement

2.2.1 Details of specimens

As described previously, in order to fabricate a truss with a concentric joint arrangement, it is necessary to remove part of the lip of one of the channel-sections (see Fig. 3) in the vicinity of the joint. In this Section, tests are described to investigate the reduced strength owing to out-of-plane buckling caused by the discontinuity of the lip (see Fig. 13). The tests are to be referred to as the truss panel tests, and are in a form of triangular truss. Fig. 9 shows details of the truss panel tests. The same channel-sections and the HRC were used for truss panel specimens. Fig. 10 shows the labelling convention of the specimens.

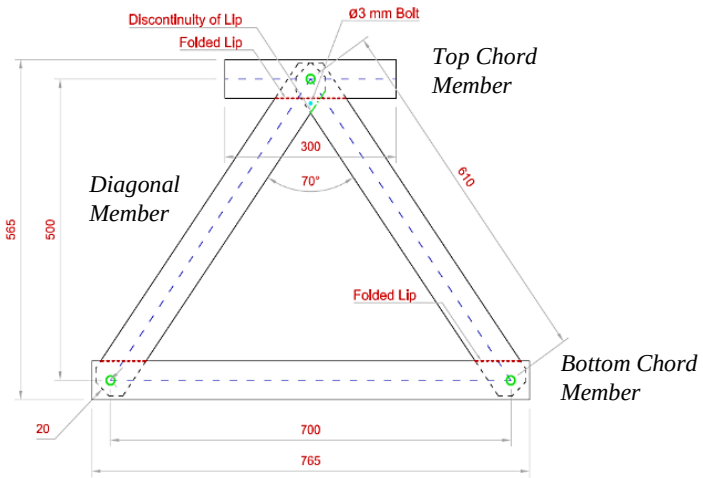

Figure 9: Truss panel specimen details

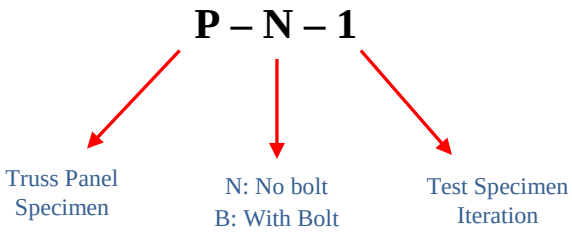

Figure 10: Truss panel specimen labeling convention

In total, four truss panel tests were conducted. In two of the truss panel tests which are referred as P-N-1 and P-N-2, only the HRC was used. In the other two truss panel tests, a 3 mm bolt was used in addition to the HRC, which are referred as P-B-1 and P-B-2.

2.2.2 Material properties

Three coupons were obtained in the longitudinal orientation and tested using the Instron Universal Testing Machine, as described in Section 2.2.1. The material properties and average test results are summarized in Table 4.

Table 4: Material properties of channel-sections (E = 230 GPa)

Nominal Thickness (mm)	Base Metal* Thickness (mm)	Gauge Width (mm)	Gauge Length (MPa)	Yield Stress (MPa)	Tensile Stress (MPa)	Elongation At Rupture (%)
0.95	0.91	20	141	710	721	1.7

*Base Metal thickness refers to ply thickness without galvanized (zinc) coating.

2.2.3 Test rig and procedure

Fig. 11 shows the truss panel test specimens mounted in the Instron Universal Testing Machine.

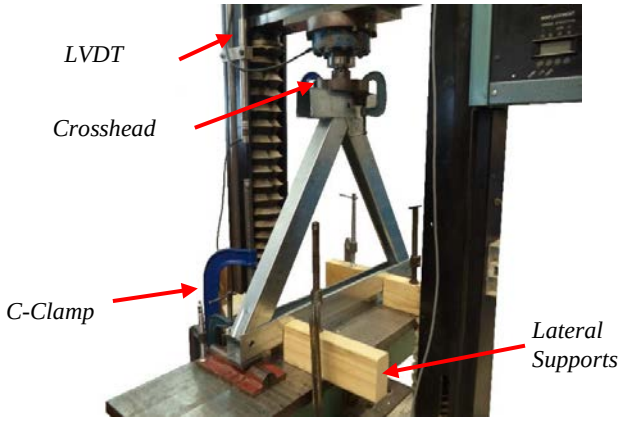

Figure 11: Truss panel specimen mounted on Instron Universal Testing Machine

The truss panel sat on top of a set of pinned supports. The truss panel centerline was aligned with the centerline of the cross head. The three corners of the truss panel were braced against out-of-plane movement. The crosshead displacement of the Instron was measured using an LVDT. The crosshead moved downwards at a constant speed of 3.0 mm/min, as specified in AISI S905 [9].

2.2.4 Test results

The experimental peak loads (P_{EXP}) of the truss panel specimens are shown in Table 5. The peak load refers to the maximum load before failure in a single diagonal member. Fig. 12 shows graphs of overall load against cross head movement. Fig. 13 shows the mode of failure.

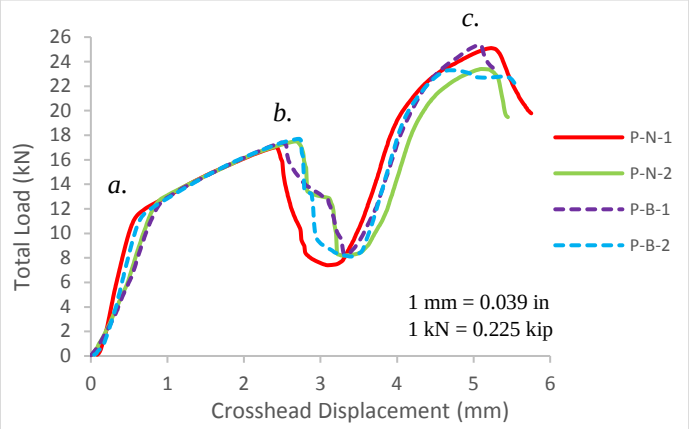

Figure 12: Total load against crosshead displacement of truss panel specimens

As can be seen from Fig. 12, there are three stages:

a. HRC reaches its yield point and begins to deform plastically (see Fig. 13a)
b. HRC squashes and the outer swaged collars shear (see Fig. 13b)
c. Load now directly transferred in bearing through the top chord to the diagonal members; peak load corresponds to diagonal member buckling out-of-plane at the discontinuity of lip (see Fig. 13c).

It can be seen from Fig. 12 and Table 5 that adding the 3 mm bolt at the discontinuity had little effect on the overall behaviour of truss panel.

a. Softening of HRC b. Squashing of HRC c. Failure of discontinuity

Figure 13: Failure modes of truss panel specimens without bolt at discontinuity

Table 5: Experimental results from truss panel tests

No	Test Specimen	DSM Result Without Lip P_{DSM-N} (kN)	DSM Result With Lip P_{DSM-L} (kN)	Total Peak Load P_{TEXP} (kN)	Peak Load in a Single Member P_{EXP} (kN)	Mean Peak Load P_{mEXP} (kN)	Variation η (%)	P_{EXP}/P_{DSM-N}	P_{EXP}/P_{DSM-L}	Mode of Failure
1	P-N-1	13.29	28.95	25.11	15.33	14.80	3.53	1.15	0.53	[1]SH + LDB
2	P-N-2			23.40	14.28			1.07	0.49	SH + LDB
3	P-B-1			25.37	15.49	14.85	4.25	1.17	0.53	[2]SH + DMB
4	P-B-2			23.30	14.22			1.07	0.49	SH + DMB
Mean P_m								1.116	0.512	
Mean Standard Deviation								0.050	0.023	
Coefficient of Variation, V_p								0.045	0.045	

[1]Squshing of HRC + Buckling of lip at discontinuity

[1]Squshing of HRC + Buckling of diagonal member

3 Analysis of Results

3.1 Frame analysis

The full-scale truss was idealised in SAP2000 [10]. The elastic load deflection obtained is also shown in Fig. 7. As can be seen, the elastic gradient predicted by the SAP2000 model is similar to the experimental results. Fig. 14 shows the axial force diagram of the full-scale truss having the concentric and eccentric joint arrangement using SAP2000. As can be seen in Fig 14, the outer diagonal members were the critical members and failed in flexural-torsional buckling as expected and observed in Fig 8. There was also no deformation or failure observed during the experiment in the inner diagonal members consistent with the force distribution from the SAP2000 model.

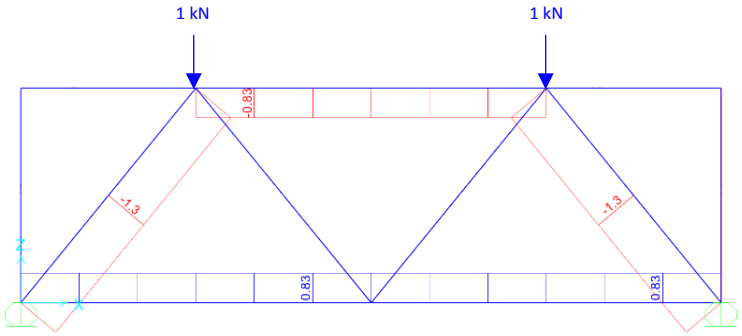

a. Concentric joint arrangement

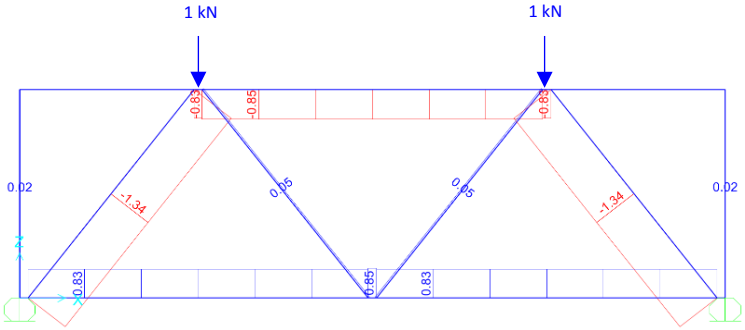

b. Eccentric joint arrangement

Figure 14: Axial force diagram of the full-scale truss specimen using SAP2000

3.2 Comparison of results against design standard

3.2.1 Truss panel

It was observed from the truss panel tests that the section failed due to discontinuity of the lip (see Fig. 13). The failure load is also plotted in Fig. 15. The analysis was implemented using Cornell University Finite Strip Method (CUFSM) software [11] and Direct Strength Method within AISI [12] and AS/NZS 4600 [13] design standards. The experimentally measured elastic modulus (E) was input in CUFSM, i.e. 230 GPa. As can be seen in Table 5, the failure load is similar to the DSM section capacity when calculated for the channel section without the lip. Only removing part of the lip at vicinity of the joint, resulted in 50% reduction in compressive strength of the member according to the DSM result. Therefore, where the elastic deflection of the system with an

eccentric joint is within the criteria of the relevant Standard, the eccentric joint arrangement is recommended for a truss assembly.

3.2.2 Full-scale truss

The member capacity of the diagonals was calculated in accordance with the DSM. Fig. 15 shows the DSM results and experimental results for the HRC. P_{EXP}/P_s refers to ratio of the experimental result to the section capacity of channel sections.

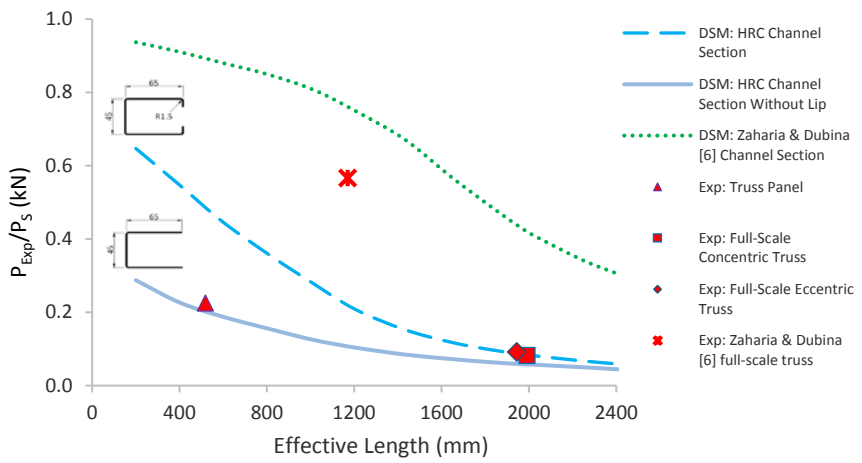

Figure 15: Experimental results for the HRC and Zaharia and Dubina [6]

For the full-scale truss, the experimental failure load of the diagonals was predicted accurately by the DSM (see Table 3) using an effective length of $0.85L_d$ and experimentally measured elastic modulus of 230 GPa. Even though the peak load was similar, the mid-span deflection of the eccentric jointed truss was 3 times larger than the concentric jointed truss due to 70 mm eccentricity of the HRCs. For reference, Table 6 shows the theoretical buckling capacities of the section calculated using Effective Width Method (EWM) [11, 12]. As can be seen, there is a good agreement between the experimental and EWM results.

Table 6: Full-scale truss results against EWM results [11, 12]

Dia. Member Length, L_d mm	Effective Length mm	Flexural-torsional Buckling, $P_{f\text{-}t}$ kN	P_{EXP} kN	$P_{EXP}/P_{f\text{-}t}$
2288	1944.80	6.01	6.02	1.00
2343	1991.55	5.75	5.42	0.94

For comparison, Fig. 15 also shows the case of the experimental tests of Zaharia and Dubina [6], which failed through flexural instability of the diagonal member. As can be seen, the failure load predicted by the DSM is slightly over conservative, because combined actions and the rotational stiffness of the bolt-group have been ignored.

4 Conclusions

This paper has described the behaviour of a cold-formed steel truss system that uses a novel pinned connector for the joints, referred to as the Howick Rivet connector (HRC). Full-scale truss tests have been described using both pinned concentric and pinned eccentric joint arrangement have been tested. It has been shown that the mid-span deflection of the concentric joint arrangement in the elastic range is 3 times smaller and 64% stiffer than that of the eccentric joint arrangement; the overall failure loads, due to flexural-torsional buckling of the diagonal members, were found to be similar, and were not influenced by removal of part of the lips of the channel-sections. To investigate the effect of removing the lips for the concentric joint arrangement, truss panel tests have been performed for which the length of the diagonals were 0.6 m. Failure was found to be localised buckling at the discontinuity where the lip was removed. The experimental strength of truss panel has been compared with the DSM; and found to be similar to the member capacity of the channel section without a lip. It is concluded that where the deflection is not a limiting factor, eccentrically jointed truss could be used to preclude compromising the member capacity by removing part of the lip at vicinity of the joint.

References

[1] Ahmadi, A, Mathieson, C, Clifton, GC, Das, R, & Lim, JBP 2016, 'An experimental study on a novel cold-formed steel connection for light gauge open channel steel trusses', *Journal of Constructional Steel Research*, vol. 122, pp. 70-79.

[2] Mathieson, C, Clifton, GC, & Lim, JBP 2016, 'Novel pin-jointed connection for cold-formed steel trusses', *Journal of Constructional Steel Research*, vol. 116, pp. 173-82.

[3] Harper, MM, LaBoube, RA, & Yu, WW 1995, 'Behavior of cold-formed steel roof trusses', *Center for Cold-Formed Steel Structures Library*, viewed 8 February, 2016, http://scholarsmine.mst.edu/ccfss-library/47

[4] Riemann, JA, LaBoube, RA, & Yu, WW 1996, 'Behavior of compression web members in cold-formed steel truss assemblies, *Center for Cold-Formed Steel Structures Library*, viewed 8 February, 2016, http://scholarsmine.mst.edu/ccfss-library/132

[5] LaBoube, RA, & Yu, WW 1998, 'Recent research and developments in cold-formed steel framing, *Thin-Walled Structures*, vol. 32, pp. 19-39.

[6] Zaharia, R, & Dubina, D 2006, 'Stiffness of joints in bolted connected cold-formed steel trusses', *Journal of Constructional Steel Research*, vol. 62, pp. 240-49.

[7] ISO E. 6892-1 2009, *Metallic materials-tensile testing-part 1: Method of test at room temperature ISO E. 6892-1*, International Standard, Geneva.

[8] Standards Australia 2011, *Australian Standard AS 1397 continuous hot-dip metallic coated steel sheet and strip--coatings of zinc and zinc alloyed with aluminium and magnesium*, Standards Australia, Sydney.

[9] AISI Standard 2008, *Test methods for mechanically fasted cold-formed steel connections AISI S905,* American Iron and Steel Institute, Washington DC.

[10] Computers & Structures, 2015, SAP2000 (version 18) [computer program]. Available at https://www.csiamerica.com/products/sap2000

[11] Li, Z, Schafer, BW 2010, 'Buckling analysis of cold-formed steel members with general boundary conditions using CUFSM: conventional and constrained finite strip methods.' *Proceedings of the 20th International Specialty Conference on Cold-Formed Steel Structures*, St. Louis, MO.

[12] AISI Standard 2012, *North American Specification for the Design of Cold-Formed Steel Structural Members AISI S100*, American Iron and Steel Institute, Washington DC.

[13] Standards Australia and New Zealand 2005, *Australian and New Zealand Standard AS/NZS 4600 Cold-formed steel structures*, Standards Australia, Sydney; Standards New Zealand, Wellington.